

Phenomenal study on the dopant activation behavior in polysilicon thin films doped by non-mass separated ion mass doping technique

Jin-Young Yoon and Duck-Kyun Choi

Department of Inorganic Materials Engineering, Hanyang University, Seoul 133-791, Korea

비질량 분리 이온 질량 주입법으로 도핑시킨 다결정 박막의 도판트 활성화 거동

윤진영, 최덕균

한양대학교 무기재료공학과, 서울, 133-791

Abstract The electrical properties of polysilicon thin films implanted with B_2H_6 diluted in H_2 as dopant source using ion mass doping technique and the effect of radiation damage on the dopant activation behavior were investigated. Comparing the SIMS profiles of boron in polysilicon films with that obtained from computer simulation using TRIM92 the most probable ion species were $B_2H_x^+$ ($x=1, 2, 3\cdots$) type molecular ions. As a result of the implantation of energetic massive ions, a continuous amorphized layer was created in polysilicon films where the fraction of amorphized layer varied with doping time. This amorphization comes from the fact that mass separation of implanting species is not employed in this ion mass doping technique. In the dopant activation behavior, reverse annealing phenomenon appeared in the intermediate annealing temperature range for a severely damaged specimen. The experimental result showed that the off-state current of the p-channel polysilicon thin film transistor is dependent on the degree of radiation damage.

요약 본 연구는 수소로 희석된 B_2H_6 를 도판트 소스 가스로 사용하여 이온 질량 주입(ion mass doping)을 하였을 때 다결정 박막의 전기적 특성과 도판트의 활성화시 방사 손상(radiation damage)의 효과에 대하여 고찰하였다. 다결정 박막에서 보론(boron)의 SIMS 분석과 컴퓨

터 시뮬레이션인 TRIM92를 비교해서 가장 주입 확률이 높은 이온의 종류는 $B_2H_x^+$ ($x=1, 2, 3\cdots$) 형태의 분자 이온임을 알았다. 높은 에너지의 질량 이온 주입 결과 시간에 따라 변화하는 비정질화된 층의 분율이 다결정 박막 내에 연속적인 비정질 층으로 존재하였다. 주입 이온의 질량 분리가 일어나지 않는 이온 질량 주입법(ion mass doping technique)에 의해 비정질화는 유발된다. 손상된 시편의 중간 열처리 온도 범위에서 도판트 활성화 거동과 역 열처리(reverse annealing) 효과가 관찰되었다. 이와 같은 연구의 결과 p-채널 다결정 박막 트랜지스터의 오프 스테이트(off-state) 전류는 방사 손상(radiation damage)에 의존한다.

1. Introduction

Ion implantation technique has been widely used in IC process since it has several advantages over the thermal diffusion process. However, it is not adequate for large-scaled microelectronics of great importance these days because ion implantation requires not only beam scanning due to its tiny beam size but also high temperature post annealing process to heal the radiation damage formed in target material. Therefore, new type of dopant implantation technique which is capable of low temperature activation and effective in large area doping has been developed [1-4]. This ion mass doping technique is especially essential for the fabrication of large area polysilicon TFT LCD (Thin Film Transistor Liquid Crystal Display)s where the process temperature is restricted below 600°C for replacing the expensive quartz plate to cost effective borosilicate glass.

Various ions are implanted through ion mass doping because this technique inherently does not separate ions [5]. Especially, the molecular ions create large amount of radiation damage in polysilicon films and, in turn,

influence the electrical properties of polysilicon thin films. In the case of boron implantation, due to its great difference in ionic mass between B^+ ion and molecular ions (B_2^+ , $B_2H_x^+$, etc.), such effects on polysilicon films remarkably differs even with identical acceleration energy. Heavy elements like arsenic and antimony are known to create amorphous layer damage along the stopping trajectories and also responsible for the formation of continuous amorphized layer above the critical dopant concentration. This damaged layer is related to the activation behavior of dopant atoms [6,7]. Since the influence of radiation damage on the electrical properties of polysilicon films becomes more important as the film thickness decreases, such phenomenon needs to be considered more carefully.

In this study, the major ion species involved in ion mass doping were traced for the polysilicon films implanted with B_2H_6 which is a common source for p-type dopant and the degree of radiation damage was examined. The variation of sheet resistance of polysilicon films with respect to annealing temperature and such effect on the current-voltage characteristics of p-channel

polysilicon thin film transistors fabricated using ion mass doping technique were also studied.

2. Experimental details

Schematic of ion mass doping system is drawn in Fig 1. The 1 % B_2H_6 gas diluted in H_2 was introduced to quartz chamber (40 cm(ϕ) \times 50 cm) and discharged by RF power (13.56 MHz). The RF power used was 100W in this work. The ions were accelerated by the applied voltage ranged from 1 kV to 20 kV and implanted for 1~30 min into 150 nm thick polysilicon films grown by LPCVD at 625°C on the top of SiO_2/Si substrate. The substrate was neither heated nor cooled during ion doping and the working pressure was kept at 1 mtorr. Ion flux was measured using a Faraday cup and was also calculated from the ion current through

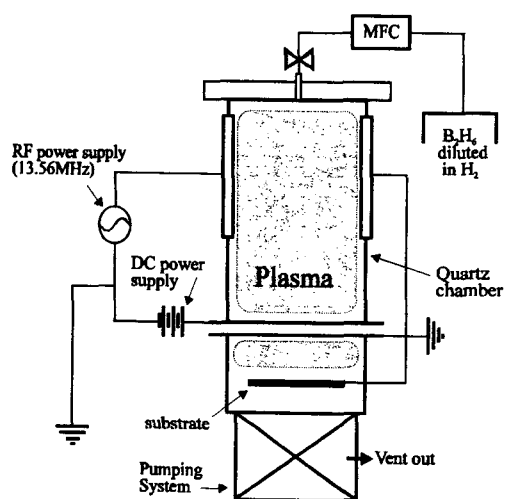


Fig. 1. Schematic diagram of ion mass doping system.

lower grid. It was dependent on the process parameters and ranged in $10\sim 20 \mu A/cm^2$.

Boron profiles in polysilicon films were analyzed by SIMS and compared to the results obtained from computer simulation using TRIM92. This program is widely used for the calculation of range distributions in ion implantation [8]. In the simulation, the profiles and projected ranges (R_p) of all the possible ions with different mass such as B^+ , B_2^+ , $B_2H_x^+$ ($x=1,2,3\cdots$) were calculated to identify the most probable species involved in ion mass doping.

Cross-sectional morphology of ion mass doped polysilicon films was examined by TEM to analyze the damage creation during ion mass doping. To study the activation behavior of dopants, furnace annealing process followed for 3 hours at $400^\circ C\sim 900^\circ C$ in Ar ambient. Sheet resistances of the films before and after annealing were measured by 4-point probe. Finally, p-channel polysilicon thin film transistors were fabricated using ion mass doping technique and the current-voltage characteristics were analyzed.

3. Result and discussion

3.1. Ion species

Figure 2 shows the SIMS profile of boron in polysilicon films for 2 min doped at 17kV and the computational profile obtained from computer simulation using TRIM92. Projected range (R_p) measured from SIMS is about 23 nm. It is quite obvious that there is a dis-

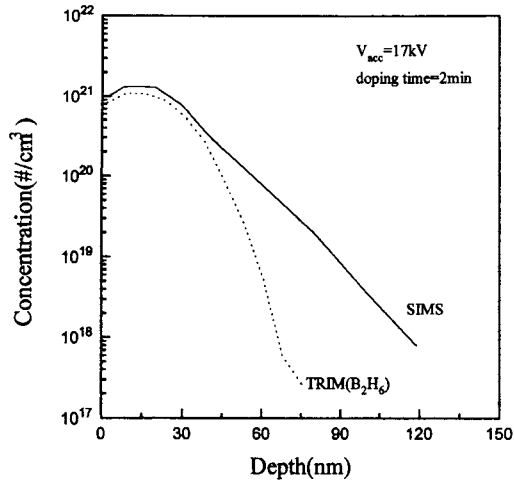


Fig. 2. Calculated range of distribution of B₂H₆ using TRIM92 and SIMS profile of boron by ion mass doping technique at the same acceleration voltage.

crepancy in R_p between ion mass doping profile and the one simulated for B⁺ (MW = 11.01 amu) ions. It turned out that the B₂H₆⁺ (MW = 28.07 amu) ion is the most probable species to generate the closest R_p . Considering the possible computational error in simulation, this result implies that the major implanted species in ion mass doping is not B⁺ ions but B₂H_x⁺ type ions. Moreover, the difference in projected straggle is believed to be from the overlap of profiles from various possible ion species such as B⁺, B₂⁺, B₂H_x⁺, etc.

Another evidence can be drawn from the hydrogen distribution in the polysilicon film plotted in Fig. 3. The hydrogen peak near the surface of polysilicon film is considered to be from B₂H₆⁺ ions since its profile follows that from B₂H₆⁺ ions.

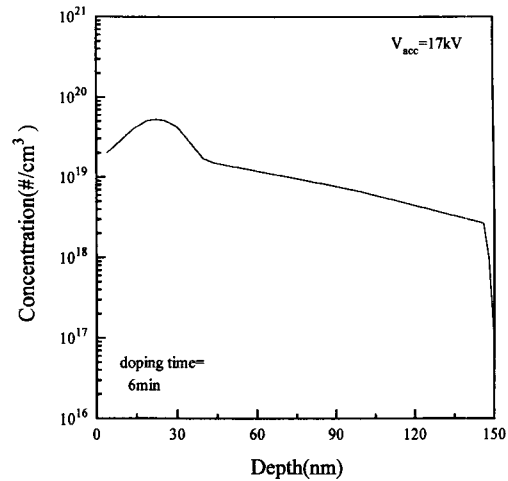


Fig. 3. SIMS profile of hydrogen in polysilicon film at 17 kV.

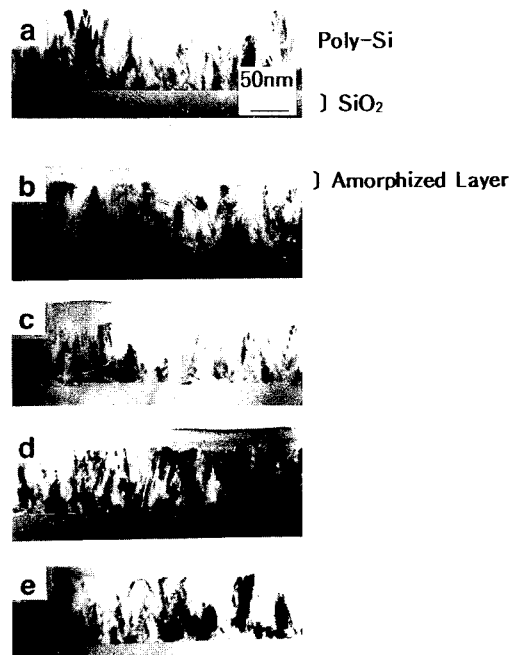


Fig. 4. Cross-sectional TEM micrographs of polysilicon films. (a) 150 nm thick polysilicon film deposited by LPCVD at 625°C on a SiO₂ layer, (b) boron implanted for 2 min by ion mass doping technique, (c) 5 min, (d) 8 min and (e) 10 min.

3.2. Radiation damage

It is expected that there would be considerable radiation damage in the polysilicon film due to the implantation of molecular ions such as $B_2H_x^+$ as in the case of heavy ion implantation. That is, the $B_2H_6^+$ ion which is heavier and bigger than B^+ ion is supposed to create severe radiation damage along the stopping trajectory in polysilicon film and even to generate an amorphized layer. Figure 4 is cross-sectional TEM micrographs of undoped and ion mass doped polysilicon films at the acceleration voltage of 17 kV for various doping times [9]. All the films indeed have a continuous amorphized layer which thickness is dependent on doping time (amount of dose). When the acceleration voltage decreased gradually from 17 to 1 kV, the amorphized layer thickness also reduced. The fraction of amorphized layer as a function of doping time is shown in Fig. 5. The thickness of amorphized layer

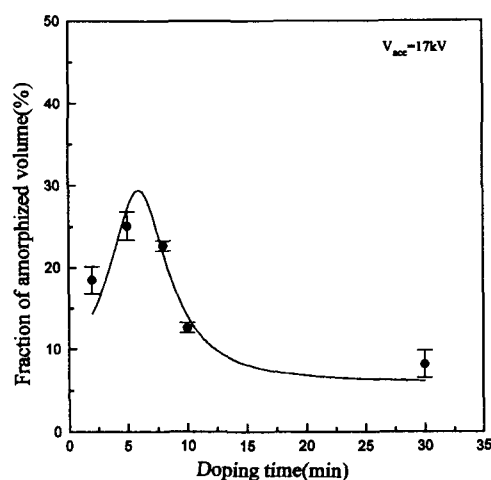


Fig. 5. Fraction of amorphized layer thickness as a function of doping time.

increases as doping time increases until 6 min and starts to decrease. For the short time doping, the thickness of amorphized layer increases because the amount of dose of respective molecular ions such as B_2^+ , $B_2H_x^+$ ($x=1, 2, 3\cdots$) reaches their amorphous threshold. Thickness of amorphized layer, however, decreases if doping time exceeds 6 min. It is considered that the substrate temperature rises when the energetic molecular ions collide to the film surface and there is a self-annealing effect during ion mass doping. In general, the recrystallization from amorphous to polycrystalline silicon occurs above 500°C [10-14]. The reason why recrystallization can happen below this temperature (about 400°C) is that the undamaged polycrystalline silicon layer plays a role as a seed layer for growth. This low temperature recrystallization has to be studied more in future. From all this consideration, the amorphized layer thickness is determined by the competition between damage creation and self-annealing effect.

3.3. Sheet resistance

The variation of sheet resistances after annealing from 400°C to 900°C is shown in Fig. 6 and it reveals three different types of annealing behavior of dopants depending on doping time (amount of dose and radiation damage). In the case of 1 min doped polysilicon film, sheet resistance exponentially decreases as the increase of annealing temperature. On the other hand, the specimen doped for 3 min shows the plateau at inter-

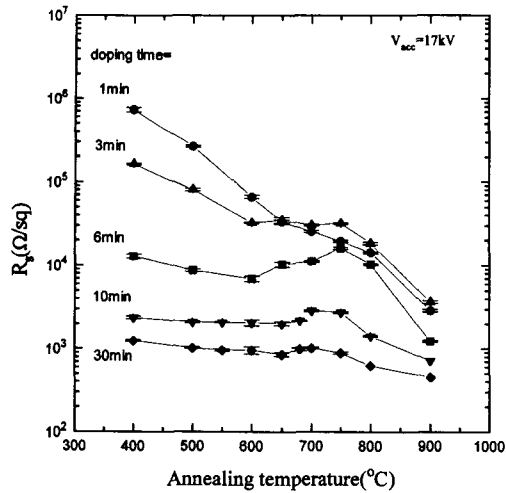


Fig. 6. Sheet resistance of polysilicon films ion mass doped for 1 min~30 min and annealed at various temperatures. The values were measured by 4-point probe before annealing process.

mediate temperature range and the awkward increase of sheet resistance occurs at the same temperature range for the 6 min doped specimen. This phenomenon is called 'reverse annealing' and will be explained later. As doping time further increases this reverse annealing effect diminishes because of the self annealing and self activation [15]. For the polysilicon film doped for 30 min, there is not a noticeable change in sheet resistance due to the saturation of self activation effect although the annealing temperature increases.

The behavior of each case in Fig. 6 can also be interpreted in terms of annealing temperatures, namely low, intermediate, and high annealing temperatures.

3.3.1. Low temperature range (400°C - 600°C)

: *short range incorporation*

For the implanted dopants being electrical-ly activated boron atoms should replace Si lattice. This process is possible with the help of diffusion. However, long range dopant diffusion is not available in this temperature range. Therefore the dopant activation is from two other possible mechanisms. One is the point defect annihilation which improves the carrier mobility and the other is the short range incorporation of boron atom and the recoiled Si into lattice.

3.3.2. Intermediate temperature range (600°C - 750°C) : *recrystallization of amorphized layer and carrier trapping by dislocation loops*

It is known that the typical temperature range for the recrystallization of amorphous silicon is 550°C ~ 650°C and dislocation loops and grain boundaries are developed at this range. The defects formed during recrystallization act as trapping centers for carriers. Therefore, the active dopant concentration decreases and sheet resistance increases as a result. This phenomenon is called 'reverse annealing' and in this experiment, it was clearly observed from the specimen doped for 6 min at 17 kV. Such effect is hard to be seen in the conventional ion implantation with B⁺ ions. Compared with the ion implantation, reverse annealing is possible in ion mass doping where the molecule-type massive ions are the main source of dopants. In this experiment, the intermediate temperature range is a region where the two opposite mechanisms occur simultaneously. The active dopant concentration de-

creases due to the trapping effect of free carriers by dislocation loops and grain boundaries formed by solid phase recrystallization while the incorporation between boron atoms and Si lattice proceed in the undamaged polysilicon layer. These two effects completely erase the influence of sheet resistance of the film doped for 3 min. For 6 min doped polysilicon film, however, the carrier trapping effect is dominant because the radiation damage is much severer than that in 3 min.

3.3.3. High temperature range (750°C - 900°C) : grain growth and long range diffusion

Generally the electrical activity of boron implanted in single crystal silicon increases until full activation is achieved at the temperature range between 800°C and 1000°C. Similarly the full activation of boron in polysilicon films due to grain growth and long range diffusion can be accomplished in this region. In Fig. 6, the sheet resistance does not decrease even though ion mass doping time increases at 900°C. This is because the increase in active dopant concentration is compensated by the decrease in carrier mobility due to the scattering between carriers [16,17].

3.4. Off-state current of polysilicon TFTs

Figure 7 shows the variation of minimum off-state currents of the p-channel polysilicon thin film transistors fabricated using ion mass doping technique as respect to the annealing temperatures. As explained previously, the electrical property of source and

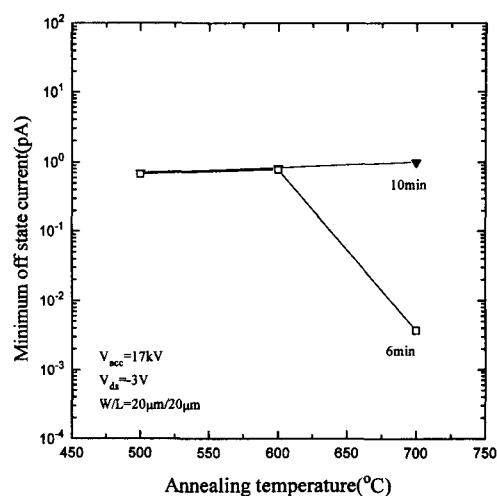


Fig. 7. Minimum off state current of 6 min and 10 min doped films at various annealing temperatures. W and L represent channel width and channel length, respectively.

drain regions of polysilicon thin film transistors is determined by the combination of radiation damage and the activated dopant concentration and such effect will leave an imprint on drain current. The minimum off-state current of polysilicon thin film transistor with the maximum radiation damage drastically decreases at 700°C which agrees with reverse annealing effect in Fig. 6. It is because the trapping effect of carriers by dislocation loops in source and drain regions. On the other hand, the self-activated polysilicon thin film transistors reveals little change in the minimum off-state current.

4. Conclusion

Ion mass doping differs from ion implantation in non-mass separation of implanting species, When B_2H_6 is chosen as a source

material, various kind of ions are implanted at the same time. Computer simulation confirms that $B_2H_x^+$ ($x=1, 2, \dots$) type molecular ions are the major sources. These heavy ions create primary radiation damage in polysilicon films and continuous amorphized layer is formed as a result. Thickness of amorphized layer is a function of doping time and acceleration voltage. The fraction of damaged layer thickness shows maximum for 6 min. doping at 17 kV. During the post annealing process 'reverse annealing' was observed in the intermediate temperature range for the specimen doped for 6 min. at 17 kV due to the carrier trapping effect by defects such as dislocation loops and grain boundaries. For the specimen doped for a long time, the sheet resistance change was not noticeable since there was enough time for activation during the implantation by self annealing.

Consequently, this study addresses the possibility of control in dopant activation behavior and the radiation damage in ion mass doping process by tuning the ion mass doping time at a given acceleration voltage. Furthermore, the self activation effect during ion mass doping promises the fabrication of low temperature polysilicon TFTs.

References

- [1] A. Yoshida, K. Setsune and T. Hirao, *Appl. Phys. Lett.* 51(4) (1987) 253.
- [2] A. Yoshida, M. Kitagawa, K. Setsune and T. Hirao, *Jpn. J. Appl. Phys.* 27 (7) (1988).
- [3] A. Mimura, G. Kawachi, T. Aoyama, T. Suzuki, Y. Nagae, N. Konishi and Y. Mochizuki, *IEEE Trans. Electron Devices* 40 (3) (1993).
- [4] Y. Wu, J.H. Montgomery, et. al., *IEEE Proc.-Circuits Devices Syst.* 141(1) (1994) 23.
- [5] Y. Mishima and M. Takei, *J. Appl. Phys.* 75 (10) (1994) 4933.
- [6] T. Motooka, et. al., *Jpn. J. Appl. Phys.*, Vol. 32, Pt. 1, No. 1B, (1993) 318.
- [7] T. Hara, K. Shinada and S. Nakamura, *Jpn. J. Appl. Phys.*, Vol. 33, Pt. 1, No. 10, (1994) 5608.
- [8] A. Yoshida, M. Kitagawa and T. Hirao, *Jpn. J. Appl. Phys.*, Vol. 32, Pt. 1, No. 5A, (1993) 2141.
- [9] H. Cerva, *J. Mater. Res.* 6(11) (1991) 2324.
- [10] C.V. Thompson, *J. Appl. Phys.* 58 (2) (1985) 763.
- [11] R.B. Iverson and R. Reif, *J. Appl. Phys.* 62 (5) (1987) 1675.
- [12] G. Carter and M.J. Nobes, *J. Mater. Res.* 6(10) (1991) 2103.
- [13] G. Shi and J.H. Seinfeld, *J. Mater. Res.* 6(10) (1991) 2091.
- [14] G. Shi and J.H. Seinfeld, *J. Mater. Res.* 6(10) (1991) 2098.
- [15] A. Yoshinouchi, A. Oda, Y. Murata, T. Morita, *Jpn. J. Appl. Phys.*, Vol. 33, Pt. 1, No. 9A, (1994) 4833.
- [16] T.I. Kamins, *J. Appl. Phys.* 42(11) (1971) 4357.
- [17] J.Y.W. Seto, *J. Appl. Phys.* 46(12) (1975) 5347.